ASSOCIATION OF SHORT-ARC OPTICAL TRACKS VIA THE DIRECT BAYESIAN ADMISSIBLE REGION: THEORY AND APPLICATION

Kohei Fujimoto[(1)], Daniel J. Scheeres[(1)], Johannes Herzog[(2)], and Thomas Schildknecht[(2)]

[(1)]*The University of Colorado at Boulder, 431 UCB ECEE 166 Boulder, CO 80309-0431 USA, Email: {kohei.fujimoto, scheeres}@colorado.edu*

[(2)]*University of Bern, Sidlerstrasse 5, CH-3012 Bern, Switzerland, Email: {johannes.herzog, thomas.schildknecht}@aiub.unibe.ch*

ABSTRACT

The direct Bayesian admissible region approach is an a priori state free measurement association and initial orbit determination technique for optical tracks. In this paper, we propose a hybrid approach that appends a least squares estimator to the direct Bayesian method. We test this approach on measurements taken at the Zimmerwald Observatory of the Astronomical Institute at the University of Bern. Over half of the association pairs agree with conventional geometric track correlation and least squares techniques. Furthermore, the number of false positive solutions is cut by more than half compared to direct Bayesian only.

Key words: space situational awareness; too-short-arc problem; measurement association; initial orbit determination; admissible region.

1. INTRODUCTION

In space situational awareness (SSA), the vast majority of observations of objects beyond low-Earth orbit are made by optical sensors, which measure a time history of angles called "tracklets" for a given object [DJS09, TMR07]. The range and range-rate, however, remains largely unconstrained, and thus multiple tracklets must be combined in order to obtain a full 6-dimensional state estimate. For short-arc observations common in survey-type observations, this task is not trivial as a large subset of the state space is consistent with any given tracklet pair. Therefore, traditional initial orbit determination (IOD) techniques often perform poorly giving rise to false correlation results and unrealistic state estimates.

The direct Bayesian admissible region approach proposed by Fujimoto and Scheeres is an *a priori* state free measurement association and IOD technique [FS12a, FS12b]. In previous work, the uncertainty of the observed object's state due to measurement errors is ignored based on the fact that the uncertainty due to the lack of knowledge in range / range-rate dominates the procedure. Further investigation in the effect of measurement errors on ARs, however, suggests that, for real-world applications, this simplification is not always justified especially when the state space discretization is refined to improve estimate accuracy. In addition, false positive associations originating from the ambiguity in the orbital period of the observed object (i.e., multi-rev solutions) are not explicitly accounted for. In this paper, we propose a hybrid approach that takes the observation association and initial orbit determination results of the direct Bayesian method and passes them to a least squares estimator. In order to better exclude multi-rev solutions, a maximum limit is set to the p-value of the simple linear regression correlation coefficient of the measurement residuals. We test the hybrid approach on 212 tracklets of geosynchronous (GEO) belt objects taken at the Zimmerwald Observatory of the Astronomical Institute at the University of Bern (AIUB) [HSP11]. The hybrid approach not only reduces the number of false positives compared to the direct Bayesian only results but also detectes more new objects. Discrepancies with geometric track correlation cast light on the fundamental limits of conducting tracklet association based solely on dynamical information.

2. BACKGROUND

In this section, necessary concepts are introduced, such as the too-short arc problem and tracklet association with the direct Bayesian admissible region. Next, observation capabilities at AIUB as well as the current procedure to process observations are discussed.

2.1. The Too-Short Arc Problem

Optical observations of RSOs only contain angular information regarding the observed objects' states; that is, per observation, the range and range-rate remain largely unconstrained. Consequently, orbit determination has traditionally been conducted with some type of batch or se-

quential estimation algorithm, whose *a priori* information is supplied via geometric techniques known as initial orbit determination (IOD) [TSB04, Val07]. Here, the association of observations must be assumed initially and then deduced from the quality of the least-squares fit; that is, the association of observations is a direct function of the quality of the orbit estimation and vice versa. This approach becomes problematic especially in a survey-type observation strategy. Usually, only a limited number of observations are available per night per object, each over short observation arcs, or *tracklets*, that span a few minutes [MSA09]. Given such a small window of data, a large subset of the state space remains consistent with each tracklet, leading to poor convergence to the true solution if not divergence. The association of tracklets, therefore, cannot be inferred confidently.

Furthermore, in order to derive tractable geometric relationships between line-of-sight vectors, a simplistic dynamical model must be incorporated in the IOD. For example, the orbit may be assumed to be circular, or the Earth's gravity field may be considered as a point mass [FSMP09]. The former fails to incorporate eccentric orbits such as those in a geostationary transfer orbit (GTO) or high area-to-mass ratio (HAMR) objects [RS12]. The latter, although valid for celestial bodies that are predominantly influenced by gravity, is less effective for RSOs which experience many perturbing forces including atmospheric drag, irregularities of the central body, and solar radiation pressure, just to name a few. These difficulties in the association of optical observations of RSOs as well as the subsequent orbit determination are referred to as the *too-short arc* (TSA) problem [MGVK04, MK05, TMR07].

2.2. The Direct Bayesian Admissible Region Approach

Various methods applying the *admissible region* (AR) concept to the TSA problem for RSOs have been studied in recent years [MSA09, TMR07, FTMR10, DJ12]. In this paper, we define the AR as a probability density function (pdf) constrained in the range and range-rate directions via a few physical criteria such as that the orbit is elliptic, the object's range is within the sensing capabilities, and so on [FS12a]. The angle and angle-rate, nominally in right ascension α and declination δ, at the epoch of a tracklet may be estimated via a least-squares fit of the tracklet data to a polynomial model in time. These variables plus necessary parameters, such as the latitude ϕ and longitude Θ of the observation point, are referred to collectively as the *attributable vector*. Thus, each point on the AR combined with the attributable vector corresponds one-to-one with a state that the observed object may have taken. Furthermore, the covariance from the least-squares fit may be incorporated in the AR to represent observational errors.

Suppose that, given some set of criteria $\mathcal{C}$, A is a compact set in state space $\mathcal{X}$ that meet $\mathcal{C}$. Then, the AR $F_{\mathcal{C}}[\mathbf{X}(t^0);\mathfrak{Y}^0]$ is a pdf over $\mathcal{X}$ assigned to an attributable vector $\mathfrak{Y}^0$ such that the probability p that the observed object exists in region $B \subset A$ at time t^0 is

$$p[\mathbf{X}(t^0)] = \int_B F_{\mathcal{C}}[\mathbf{X}(t^0);\mathfrak{Y}^0]\mathrm{d}X_1^0\mathrm{d}X_2^0\ldots\mathrm{d}X_n^0, \quad (1)$$

where $\mathbf{X}(t^0) \in \mathcal{X}$ and

$$\mathbf{X}(t^i) \equiv \mathbf{X}^i = (X_1^i, X_2^i, \ldots, X_n^i). \quad (2)$$

Note that we impose $\int_A F_{\mathcal{C}}[\mathbf{X}(t^0);\mathfrak{Y}^0]\mathrm{d}\mathbf{X}^0 = 1$. In this paper, the criteria are

$$\mathcal{C} = \bigcap_{i=1}^{4} \mathcal{C}_i, \quad (3)$$

and

$$\mathcal{C}_1 = \{(\rho,\dot\rho) : E \le 0\} \quad (4)$$
$$\mathcal{C}_2 = \{(\rho,\dot\rho) : 1.03 \le \rho \le 8.53, -5 \le \dot\rho \le 5\} \quad (5)$$
$$\mathcal{C}_3 = \{(\rho,\dot\rho) : 1.03 \le r_p\} \quad (6)$$
$$\mathcal{C}_4 = \{(\rho,\dot\rho) : r_a \le 15\}. \quad (7)$$

where E is the specific geocentric energy of the particle, and r_a and r_p are the apoapsis and periapsis radii of the orbit, respectively. Units of length are in Earth radii and time in hours. These criteria ensure that the AR encompasses most trackable object relevant to SSA while simultaneously filtering out highly eccentric orbits.

We may apply Bayes' rule directly to ARs in a common state space and at a common epoch τ; no reference state is required. To obtain the posterior pdf $h[\mathbf{X}(\tau)]$ based on two ARs $F_{\mathcal{C}}[\mathbf{X}^1;\mathfrak{Y}^1]$ and $F_{\mathcal{C}}[\mathbf{X}^2;\mathfrak{Y}^2]$,

$$h[\mathbf{X}(\tau)] = \frac{\{\mathcal{T}(\tau,t_1)\circ F_{\mathcal{C}}[\mathbf{X}^1;\mathfrak{Y}^1]\}\{\mathcal{T}(\tau,t_2)\circ F_{\mathcal{C}}[\mathbf{X}^2;\mathfrak{Y}^2]\}}{\int\{\mathcal{T}(\tau,t_1)\circ F_{\mathcal{C}}[\mathbf{X}^1;\mathfrak{Y}^1]\}\{\mathcal{T}(\tau,t_2)\circ F_{\mathcal{C}}[\mathbf{X}^2;\mathfrak{Y}^2]\}\mathrm{d}\mathbf{X}}, \quad (8)$$

where $\mathcal{T}(\tau,t^i)$ is a transformation that maps some pdf $f(\mathbf{X}^i,t^i)$ from time t^i to τ, and $\mathbf{X}(\tau) \equiv \mathbf{X}$. The domain of integration is over the entire state space. Note that, in general, any pdf may be used as input, such as density information from debris distribution models [OSW$^+$06]. This direct approach is computationally feasible because each AR, ignoring observation errors, has codimension 4, making the problem extremely sparse. Furthermore, the sparseness also ensures that misassociations are highly unlikely unless the association is consistent with both the observation geometry and the dynamics [Car95]. From the Theorem of General Position, $h[\mathbf{X}(\tau)] = 0$ for all $\mathbf{X}$ generically if

$$\dim\{F_{\mathcal{C}}[\mathbf{X}^1;\mathfrak{Y}^1]\} + \dim\{F_{\mathcal{C}}[\mathbf{X}^2;\mathfrak{Y}^2]\} < \dim(\mathcal{X}), \quad (9)$$

where $\dim(\mathcal{X})$ is the dimension of the state space. Again, ignoring observation errors, $\dim\{F_{\mathcal{C}}[\mathbf{X}^i;\mathfrak{Y}^i]\} = 2$ so the inequality holds for $\dim(\mathcal{X}) > 5$. The justification of associations is not at all related to the OD quality but rather solely by the geometry of the AR maps; therefore, this method is robust with minimal tuning. Finally, transformation $\mathcal{T}(\tau,t^i)$ is expressed analytically by means of

Figure 1. Current setup of ZimSMART [HSP11].

a special solution to the Fokker-Planck equations valid for all deterministic dynamical models. Given solution flow $\mathbf{X}(t) = \boldsymbol{\phi}(t; \mathbf{X}^i, t^i)$ to the dynamics for initial conditions $\mathbf{X}^i$, the pdf $\mathcal{T}(\tau, t^i) \circ f(\mathbf{X}^i, t^i) = f(\mathbf{X}, \tau)$ is expressed as

$$f(\mathbf{X}, \tau) = f[\boldsymbol{\phi}(\tau; \mathbf{X}^i, t^i), \tau] = f(\mathbf{X}^i, t^i) \left| \frac{\partial \mathbf{X}(\tau)}{\partial \mathbf{X}^i} \right|^{-1}, \quad (10)$$

where $|\cdot|$ indicates the determinant operator.

2.3. Optical Observation Capabilities And Processing at AIUB

The Zimmerwald observatory, located about 10km south of Berne, Switzerland (46.8772 N, 7.4652 E; altitude 951.2 m), consists of several optical telescopes [HSP11, HFS10, FSMP09]. One of them, the Zimmerwald SMall Aperture Robotic Telescope (ZimSMART), is best suited for surveying the sky searching for space debris; a photograph is given in Figure 1. ZimSMART is used to develop an orbital elements catalog. Two different orbital regions are surveyed: the GEO ring and the Medium Earth Orbit region (MEO). The aim of the surveys of the GEO ring is maximum coverage of the region around the celestial equator which can be observed from Zimmerwald.

Once tracklets are extracted from images, the identification of objects is performed in three steps. First, each tracklet is correlated with the JSpOC two-line element (TLE) catalog and an internal AIUB catalog via positions and velocities. The complete procedures are described in detail in [FSMP09]. In the second step, the leftover tracklets are tested pairwise to check if some of them belong to the same object; if so, they are stored as combined tracklets. Tracklets, for which no other fitting tracklet could be found, remain single. This procedure reduces the amount of computations in the following step. In the last step of the object identification process, the orbital elements of objects in the AIUB internal catalog are compared with those of the new combined and single tracklets. This method is very effective for newly detected objects with observations of only one night. More details are described in [HFS10]. The identifications via positions and velocities as well as those via orbital elements have to be confirmed by a statistical orbit determination (OD). The new tracklet is associated with an internal catalog object only if the OD is successful; i.e., if the RMS of the residuals of a least squares batch filter is below 1.5 arcsec. Due to the tracklets being *too short arc* and lacking dynamical information, especially when the tracklet pairs span a single night, not every Keplerian element is included in the RMS, but rather only the semi-major axis, inclination, and right ascension of the ascending node.

3. METHOD

In order to ascertain validity in real-world observing scenarios, the direct Bayesian approach is applied to optical tracks taken with the ZimSMART telescope. In this section, the methodology from the observation to the orbit estimate end-product is discussed. Two potential difficulties are anticipated with the nominal assumption that the observation errors are small enough to be ignored. The first is that the zero-error assumption can cause missed associations when the state space discretization is refined to a level practical for IOD purposes. The extension of the two-dimensional linear map extrapolation discussed in [FS12b] proves to be too computationally expensive for this particular problem. The second is that the ambiguity in the number of revolutions the observed object potentially made between two tracklet pairs leads to a large number of false associations. A theoretical explanation of these fictitious solutions, or *multi-rev* solutions, is given in [FS12a].

We begin by discussing the strategy with which tracklets are obtained; especially how the RA-DEC space and time are discretized. Next, as a solution to the two difficulties mentioned previously, a "direct Bayesian + least squares" hybrid algorithm is presented.

3.1. Optical Observation Strategy

Surveys of the geostationary ring are executed by scanning declination stripes with fixed right ascension. These observations are taken without a priori information of any catalog objects. For the survey from which data processed in this chapter is extracted, 24 stripes are taken separated by 1 hour in right ascension. These stripes are at 0 hr, 1hr, . . . , 23 hr. Each stripe contains five fields separated in declination by the field of view, and similarly, five images are taken for each field. The declination of the lowest field depends on the known density of RSOs. The advantage of this method is that the observations can be acquired in a fully automated fashion with no human interaction; that is, the telescope software chooses the visible fields automatically. A tracklet contains a minimum of three images and a maximum of five, corresponding to the number of images taken per field. Depending on the

exposure time and the number of images, a tracklet thus spans anywhere between $1 \sim 2$ minutes.

3.2. Proposed "Direct Bayesian + Least Squares" Hybrid Approach

Here, we propose a hybrid approach that takes the tracklet association and initial orbit determination results of the direct Bayesian method and passes them to a least squares estimator. Although the steps in this new process are similar to those in a traditional IOD [Beu05], the justification of the association and the estimation are separated, thus improving robustness. The least squares step ensures good estimate precision without having to use a fine discretization of the state space, minimizing negative effects of measurement error on tracklet association using ARs. Furthermore, in order to better exclude multi-rev solutions, a minimum limit $p_{\min}$ is set to the p-value associated with the model utility test of the $O-C$ residuals. Suppose that for n pairs of samples $y_1, \ldots, y_n$ each associated respectively to independent variable $x_1, \ldots, x_n$, the samples are modeled with a simple linear regression model as

$$\hat{y}_i = \hat{\beta}_0 + \hat{\beta}_1 x_i, \tag{11}$$

for all integers $1 \leq i \leq n$, where the hat symbolizes that it is a model estimate. Then, for the hypothesis test regarding slope parameter β_1

$$\begin{cases} H_0 : \beta_1 = 0 \\ H_1 : \beta_1 \neq 0, \end{cases} \tag{12}$$

where H_0 is the null and H_1 the alternative hypothesis, the probability of falsely rejecting H_0 is set to be $p_{\min}$. Through this step, a maximum bound is effectively set for β_1 itself, meaning the residuals must be unbiased to time in a linear sense for an tracklet pair to be associated to a state estimate. The best estimate for the slope parameter $\hat{\beta}_1$ is

$$\hat{\beta}_1 = \frac{n\sum x_i y_i - (\sum x_i)(\sum y_i)}{n\sum x_i^2 - (\sum x_i)^2}, \tag{13}$$

where the summation is from $i = 1$ to n. Although it is not always the case that $\beta_1 = 0$ if the residuals are unbiased in time, since the tracklets arcs are so short, we can assume that the residual bias is linear enough for us to use slope parameter β_1 in this context. The test statistic is Student's t-distribution

$$t = \hat{\beta}_1 \sqrt{\frac{n(n-2)}{n\sum y_i^2 - (\sum y_i)^2 + \hat{\beta}_1(\sum x_i)(\sum y_i) - n\hat{\beta}_1 \sum x_i y_i}}. \tag{14}$$

We now present an outline of the hybrid algorithm. First, the time history of right ascension and declination must be converted into an attributable vector at the tracklet epoch; i.e. a single set of angles and angle-rates. The measured angles are fit to a polynomial kinematic model in time, such as for the right ascension

$$\alpha(t) = \alpha^0 + \dot{\alpha}^0(t-t^0) + \frac{1}{2}\ddot{\alpha}^0(t-t^0)^2, \tag{15}$$

where superscript 0 denotes the state at the tracklet epoch [MSA09]. Next, admissible regions are computed for each attributable vector in the Poincaré orbit element space. As discussed in [FS12a], the admissible region is divided into 375,000 subsets (750 units of discretization in the range-direction $\times$ 500 units in the range-rate) and each subset linearly extrapolated. The Poincaré space, and consequently the ARs, are discretized such that the bounds of the state space are

$$\mathbf{X}_{\min} = (4.5285, 0, -3, -3, -4, -4) \tag{16}$$

$$\mathbf{X}_{\max} = (14.110, 6.2832, 3, 3, 4, 4), \tag{17}$$

where the units are in Earth radii - kg - hr. The bin size is set such that the sides are $1.1052 \cdot 10^{-2}$ ($\mathfrak{L}$), $1.7453 \cdot 10^{-2}$ ($\mathfrak{l}$), $1.6667 \cdot 10^{-2}$ ($\mathfrak{G}$, $\mathfrak{g}$), and $2.2222 \cdot 10^{-2}$ ($\mathfrak{H}$, $\mathfrak{h}$) for a total of 5.2424×10^{15} bins over the entire space. This resolution corresponds to approximately 100 km in the semi-major axis direction and 1 degree in the mean anomaly direction. The admissible regions are propagated to a common epoch, which is chosen to be the tracklet epoch of the first tracklet, under two-body dynamics. The two-body assumption is made only to simplify the problem and is not central to the direct Bayesian technique.

To avoid the high computational cost of all-on-all association, the posterior pdf $h[\mathbf{X}(\tau)]$ based on the admissible regions is computed for tracklet pairs in reverse chronological order (i.e. for a set of N tracklets ordered by epoch, Tracklet 1 + Tracklet N, Tracklet 1 + Tracklet $N-1$, ...) until we find a pair for which $h[\mathbf{X}(\tau)] > 0$ [FS12a]. We then temporarily claim these tracklets as associated and run a bank of least squares filters simultaneously to refine the fit of the measurements to the state estimate. Note that if an object catalog exists, then one should first correlate tracklets with these objects first. Also, only tracklet pairs whose epochs are separated by at least 24 hours are considered so that enough dynamical information is available.

The reference state of each filter is the centroid of each bin where $h[\mathbf{X}(\tau)] > 0$ transformed into the J2000 cartesian space. In this paper, we assume that no *a priori* information exists; if desired, the *a priori* covariance may be set to approximate $h[\mathbf{X}(\tau)]$. The assumed observation error is set to 2 arcsec 1-σ. The observation-state relationship and corresponding linear partials matrix assume a spherical Earth

$$x = \rho \cos\alpha \cos\delta \tag{18}$$

$$y = \rho \sin\alpha \cos\delta \tag{19}$$

$$z = \rho \sin\delta. \tag{20}$$

For the set of filters that converge, if

1. the root mean square (RMS) of the $O-C$ residuals for both the right ascension and declination over all tracklets processed is less than some maximum $\mathrm{RMS}_{\max}$ AND
2. the p-value of the model utility test for both the right ascension and declination for each individual tracklet is greater than some minimum $p_{\min}$,

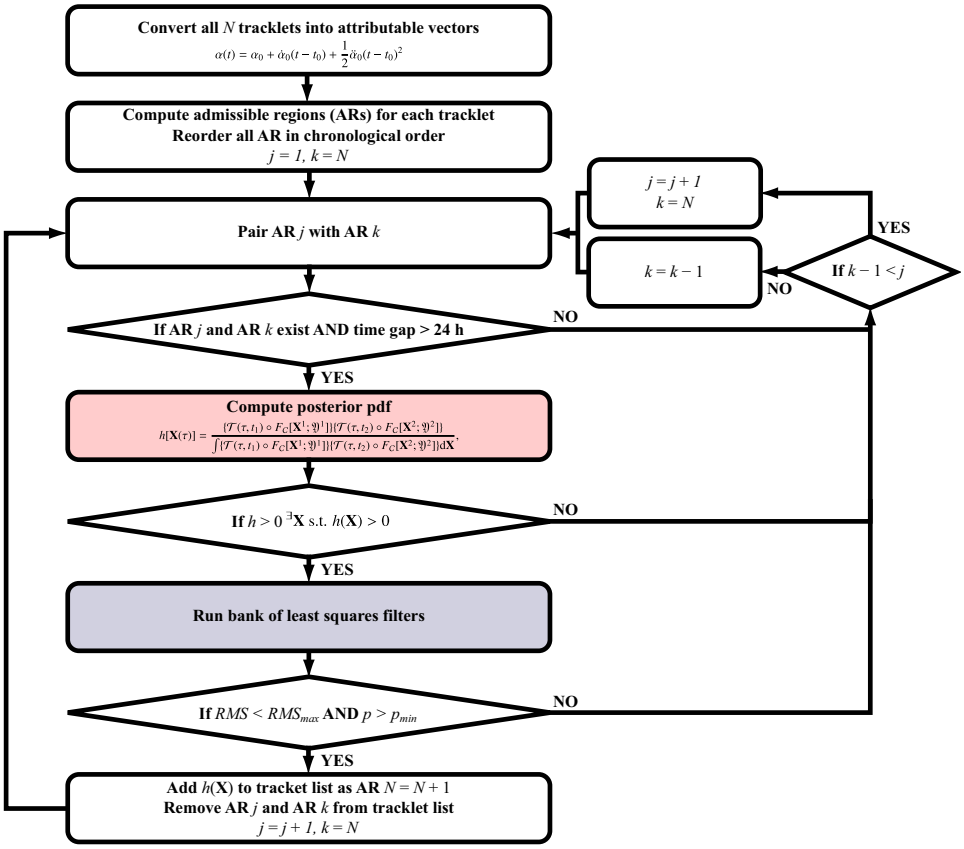

Figure 2. A flowchart of the "direct Bayesian + least squares" hybrid approach.

then the tracklets are confirmed to be associated and the state estimate with the smallest $O - C$ residual RMS is added to the object catalog. In this paper, $\mathrm{RMS}_{\max} = 0.7$ arcsec and $p_{\min} = 0.1$; these values are chosen to best describe the observational capabilities of ZimSMART. Finally, the next tracklet in the set is paired with other tracklets as before, and the process is repeated until all tracklets are processed. Figure 2 is an overall flowchart.

4. RESULTS

In this section, the outcome of tracklet association via the direct Bayesian only approach and hybrid approach are compared. We process a set of tracklets taken with the ZimSMART telescope over one RA fence; detailed measurement parameters are given in Table 1. Necessary parameters for both methods are given in Section 3.2 except that for the direct Bayesian only case, the discretization is refined dynamically over the support of the posterior pdf to $6.1449 \cdot 10^{-4}$ ($\mathfrak{L}$), $1.7453 \cdot 10^{-2}$ ($\mathfrak{l}$), $3.3333 \cdot 10^{-3}$ ($\mathfrak{G}$, $\mathfrak{g}$), and $4.4444 \cdot 10^{-3}$ ($\mathfrak{H}$, $\mathfrak{h}$) for a total of 5.8928×10^{19} bins over the entire space. The refinement guarantees that the initial orbit determination reaches practical accuracy. The solutions are then categorized into three types:

Type I The solution is most likely a true solution: associates tracklets that are also similarly correlated with the AIUB code.

Type II The solution is most likely a false positive (multi-rev) solution: associates tracklets that are correlated to two separate objects with the AIUB code AND the solution does not exist at or near ($\pm$ 200 km) GEO altitude.

Type III The solution is most likely a new true solution: at least one of the associated tracklets are not correlated with the AIUB code AND the solution exists at or near GEO altitude.

Table 2 tabulates how many solutions are found of each solution type. As expected, for the direct Bayesian only case, over 60% of the solutions found are multi-rev solutions. This ratio improves to 35% for the hybrid case; furthermore, 2 additional "true" solutions are detected. If an object is indeed observed twice or more, the fact that more multi-rev solutions are rejected means that their tracklets are not "used up" before being properly associated. All solutions obtained with the hybrid method are listed in Appendix A. Based on these results, in a real-world scenario where hundreds of tracklets that contain measurement errors are to be associated, we recommend modifying the direct Bayesian admissible region approach so that it explicitly accounts for errors as well as reduces multi-rev solutions.

Table 1. Parameters for the data set used in this paper. # of objects detected is based on AIUB correlation results.

Parameter	Value
Epoch of Initial Field	Aug 18, 2012 22:59:08.64 UTC
Epoch of Final Field	Aug 20, 2012 02:01:32.69 UTC
Total # of Field	55
Total # of Tracklets	212
Total # of Objects Detected	48
# of Objects Detected Twice w/ 24h Gap	19

Table 2. Orbit solutions found by type (I, II, or III) and association method. Δ is the difference between methods, and bold numbers indicate an improvement.

	I	II	III	Total
Direct Bayesian only	10	18	1	29
Hybrid	11	7	2	20
Δ	**+1**	**-11**	**+1**	-9

The proposed idea of applying a least squares batch filter to the direct Bayesian probabilistic output is effective but nonetheless can still be improved. Type II solutions are not completely rejected; consequently, of the 19 objects expected to be detected based on the AIUB correlation results, about 15% are missed due to one or more of their tracklets being associated to a multi-rev solution. Ruling out apparent multi-rev solutions as false associations given just the two tracklets and dynamical system flow may be difficult, especially when the measurement residuals are so well behaved. Note that multi-rev solutions are not a problem in the AIUB code as the tracklets are never associated beyond a single night. This approach is not ideal either: as discussed in Section 2.1, a lack of dynamical information can also lead to poor association solutions. Indeed, new objects within the GEO belt are detected with the hybrid approach where the associated tracklets are separated by at least 24 hours. The easiest way to reject multi-rev solutions is to conduct follow-on observations based on the estimated state. Alternatively, one can fuse some *a priori* information, such as the JSpOC TLE catalog, or information that is not of dynamical nature, such as photometry from the CCD image files [SW09, SVKE09].

Additionally, about 25% of the 19 expected objects are completely missed by the hybrid approach. In almost all of these solutions, the p-value limit for the model utility test of the $O - C$ residuals is triggered most probably by mistake. As such, we believe there exist observation scenarios where reliably evaluating the "no linear relationship" null-hypothesis can be difficult due to the small number of individual angle measurements included in a tracklet. Increasing measurements per tracklet not only will shed better light on any biases present in the residuals but also has the added benefit of improving the angle-rate estimate in the attributable vector. As shown here, because the theory discussed in this paper addresses the TSA problem in a much more probabilistically straightforward way than other IOD techniques, it allows one to reevaluate future observational strategies so that they minimize false positive / negative solutions.

5. CONCLUSIONS

In this paper, the direct Bayesian admissible region approach to short-arc association and initial orbit determination is applied to optical observations taken at the Astronomical Institute of the University of Bern. Traditional methods rely on the quality of the orbit determination to conduct observation association, which is often unreliable. The direct Bayesian approach improves robustness by leveraging the sparseness of probability distributions that describe range and range-rate ambiguity given a single optical track. Furthermore, a hybrid approach that appends a least squares batch filter is found to efficiently incorporate measurement error and reduce false positives due to multi-rev solutions. Processing a set of 212 tracklets results in 20 objects detected; 2 of which are newly detected by the proposed method. Although the hybrid approach cuts the number of false positive solutions by more than half compared to direct Bayesian only, ideas to further reject multi-rev solutions are proposed. Future work is to implement these ideas, such as increasing the number of angle measurements per tracklet, as well as further testing of the hybrid approach with more data sets.

REFERENCES

Beu05. G. Beutler. *Methods of Celestial Mechanics Volume I: Physical, Mathematics, and Numerical Principles*. Astronomy and Astrophysics Library. Springer-Verlag, Berlin, Germany, 2005.

Car95. J. S. Carter. *How Surfaces Intersect in Space: An introduction to topology*. World Scientific, Singapore, second edition, 1995. pp. 277.

Dev95. J. L. Devore. *Probability and Statistics for Engineering and the Sciences*. Wadsworth Publishing Company, Belmont, CA, USA, 4th edition, 1995.

DJ12. K. J. DeMars and M. K. Jah. Initial orbit determination via gaussian mixture approximation of the admissible region. 2012. Presented at the AAS/AIAA Spaceflight Mechanics Meeting, Charleston, SC, AAS 12-260.

DJS09. K. J. DeMars, M. K. Jah, and P. W. Schumacher. The use of short-arc angle and angle rate data for deep-space initial orbit determination and track association. 2009. Presented at the Eighth US/Russian Space Surveillance Workshop, Wailea-Maui, HI.

FS12a. K. Fujimoto and D. J. Scheeres. Correlation of optical observations of earth-orbiting objects and initial orbit determination. *Journal of Guidance, Control, and Dynamics*, 35(1):208–221, 2012.

FS12b. K. Fujimoto and D. J. Scheeres. Non-linear bayesian orbit determination: Angle measurements. 2012. Presented at the *63rd International Astronautical Congress*, Naples, Italy. IAC-12-C1.6.11.

FSMP09. C. Früh, T. Schildknecht, R. Musci, and M. Ploner. Catalogue correlation of space debris objects. 2009. Presented at the *Fifth European Conference on Space Debris*, Darmstadt, Germany.

FTMR10. D. Farnocchia, G. Tommei, A. Milani, and A. Rossi. Innovative methods of correlation and orbit determination for space debris. *Celestial Mechianics and Dynamical Astronomy*, 107(1-2):169–185, 2010.

HFS10. J. Herzog, C. Früh, and T. Schildknecht. Build-up and maintenance of a catalogue of GEO objects with ZimSMART and ZimSMART 2. 2010. Presented at the *61st International Astronautical Congress*, Prague, Czech Republic. IAC-10.A6.5.2.

HSP11. J. Herzog, T. Schildknecht, and M. Ploner. Space debris observations with ZimSMART. 2011. Presented at the *European Space Surveillance Conference*, Madrid, Spain.

MGVK04. A. Milani, G. Gronchi, M. Vitturi, and Z. Knežević. Orbit determination with very short arcs. i admissible regions. *Celestial Mechanics and Dynamical Astronomy*, 90:57–85, 2004.

MK05. A. Milani and Z. Knežević. From astrometry to celestial mechanics: orbit determination with very short arcs. *Celestial Mechanics and Dynamical Astronomy*, 92:118, 2005.

MSA09. J. M. Maruskin, D. J. Scheeres, and K. T. Alfriend. Correlation of optical observations of objects in earth orbit. *Journal of Guidance, Control and Dynamics*, 32(1):194–209, 2009.

OSW+06. M. Oswald, S. Stabroth, C. Wiedemann, P. Wegener, H. Klinkrad, and P. Vörsmann. ESA's MASTER 2005 debris environment model. *Advances in the Astronautical Sciences*, 123(1):811–824, 2006.

RS12. A. Rosengren and D. Scheeres. Long-term dynamics of HAMR objects in HEO. 2012. Presented at the *AIAA/AAS Astrodynamics Specialist Conference*, Minneapolis, Minnesota, AIAA 2012-4745.

SVKE09. T. Schildknecht, A. Vananti, H. Krag, and C. Erd. Reflectance spectra of space debris in GEO. 2009. Presented at the *Advanced Maui Optical and Space Surveillance Technologies Conference*, Wailea-Maui, HI.

SW09. R. L. Scott and B. Wallace. Small-aperture optical photometry of Canadian geostationary satellites. *Can. Aeronaut. Space J.*, 55(2):41–53, 2009.

TMR07. G. Tommei, A. Milani, and A. Rossi. Orbit determination of space debris: admissible regions. *Celestial Mechanics and Dynamical Astronomy*, 97:289–304, 2007.

TSB04. B. D. Tapley, B. E. Schutz, and G. H. Born. *Statistical Orbit Determination*. Elsevier Academic Press, Burlington, MA, 2004. pp. 159-284.

Val07. D. Vallado. *Fundamentals of Astrodyamics and Applications*. Microcosm Press, Hawthorne, CA, third edition, 2007.

APPENDIX A: STATE ESTIMATES OF OBJECTS DETECTED WITH HYBRID APPROACH

Table 3. Keplerian orbital elements of all objects detected with the hybrid approach: semi-major axis (a), eccentricity (e), inclination (i), right ascension of the ascending node (Ω), argument of periapsis (ω), and mean anomaly (M). Solutions sorted by the epoch of the first tracklet. "Tr 1" and "Tr 2" indicate the objects that the associated tracklets are correlated to by the AIUB code. Objects in the JSpOC TLE catalog are denoted by their 6 letter international designator, those in AIUB's internal catalog by a 7 letter designator starting with "Z," and uncorrelated tracks by a bracketed number assigned by tracklet epoch. "Type" is the solution type: I, II, or III.

Obj #	a **[km]**	e	i **[rad]**	Ω **[rad]**	ω **[rad]**	M **[rad]**	**Tr 1**	**Tr 2**	**Type**
1	42167.9389	0.00504009	0.15268036	0.67247208	0.67106167	4.62098602	[3]	Z12230C	III
2	42553.9802	0.00220195	0.14845483	1.02426359	-2.9210019	1.58577527	94022A	94022A	I
3	42474.7078	0.00104508	0.05504329	1.20373515	0.46646274	4.33420972	93078B	93078B	I
4	20370.2703	0.57401358	0.04134642	-1.4298436	-2.0797513	3.30584577	10032B	98050A	II
5	42167.8135	0.00485164	0.00833985	1.41736384	-0.1245722	4.65738998	00081A	00081A	I
6	44103.7561	0.03316462	0.00274204	1.53057116	-1.8511525	6.26491311	98050A	09008B	II
7	20367.0045	0.60109671	0.07350824	-2.8500348	-0.3679198	2.27664978	00054A	10025A	II
8	42166.739	0.00031368	0.00169132	0.99188551	2.49933109	2.45658423	[13]	[120]	III
9	20489.5672	0.56649625	0.04421714	-2.3842792	-0.9701911	2.77169499	08065B	10021A	II
10	26695.5358	0.38589704	0.02869554	-1.0047144	-2.714267	3.61614499	11041A	98057A	II
11	42358.4502	0.00639731	0.12502374	1.02260295	-2.8554889	1.46486536	91075A	91075A	I
12	42166.1451	0.00504257	0.00645396	1.49216639	2.92711687	1.43573959	02015B	02015B	I
13	42165.7048	0.00465978	0.00503632	-0.1067257	-1.8389239	1.53631869	98006B	98006B	I
14	42166.3074	0.00442969	0.00214473	2.01311262	2.3699257	1.51251347	10025A	10025A	I
15	42165.9793	0.00151075	0.00235757	1.3716077	3.06449675	1.4651209	08034B	08034B	I
16	42166.089	0.00093822	0.00177328	1.16793164	0.5203132	4.20931434	98057A	98057A	I
17	42369.2386	0.00313633	0.23807355	0.57337329	0.69360244	4.30588617	85015B	85015B	I
18	27240.5471	0.34495023	0.01671134	-1.7512588	-1.6627614	2.29904061	04008A	98024A	II
19	42359.0222	0.01589573	0.18605515	0.58086998	-2.3777622	0.8033633	Z11003C	Z11003C	I
20	26755.2517	0.38458146	0.03241271	-0.879943	-2.7948581	2.30041338	01042A	Z12230G	II